A Comparative Study of the Adsorption of Chloro- and Non-Chloro-Containing Organophosphorus Compounds on WO3

ARTICLE *in* THE JOURNAL OF PHYSICAL CHEMISTRY B · AUGUST 2002

Impact Factor: 3.3 · DOI: 10.1021/jp014647x

3 AUTHORS, INCLUDING:

Sofian M. Kanan
American University of Sharjah
49 PUBLICATIONS **1,082** CITATIONS

SEE PROFILE

A Comparative Study of the Adsorption of Chloro- and Non-Chloro-Containing Organophosphorus Compounds on WO_3

Sofian M. Kanan,[†] Zhixiang Lu,[†,‡] and Carl P. Tripp*[,†,‡]

Laboratory for Surface Science & Technology, and Department of Chemistry, University of Maine, Orono, Maine 04469

Received: December 31, 2001; In Final Form: July 19, 2002

The adsorption of dimethyl methylphosphonate (DMMP), trimethyl phosphate (TMP), and methyldichlorophosphate (MDCP) on monoclinic tungsten oxide (m-WO_3) evacuated at various temperatures was investigated using infrared spectroscopy. DMMP is the most common molecule used for evaluating the performance of WO_3 and other semiconducting metal oxide (SMO)-based sensors to phosphonate-based nerve agents. However, toxic nerve agents such as sarin differ from DMMP in that they contain a functional group (P−F in sarin) that can be readily hydrolyzed. It is shown that the adsorption of organophosphates that contain P−Cl groups differs from nonhalogenated simulants such as DMMP and TMP on WO_3 surfaces. Specifically, the nonchlorinated simulants DMMP and TMP adsorb on the surface solely through the P═O functionality with the surface water layer as well as the Lewis and Brønsted acid sites. The relative number of molecules bound on Lewis and Brønsted acid surface sites depends on the initial evacuation temperature of the WO_3 surface. When MDCP adsorbs on WO_3 through the P═O bond, it is accompanied by the hydrolysis of P−Cl groups by water vapor or the adsorbed water layer leading to additional phosphate-like species on the surface. The infrared data suggests that a halogenated phosphate like MDCP is a better simulant molecule for studies aimed at understanding the role of water and hydrolysis in the response of metal oxide-based sensors to nerve agents.

Introduction

Research aimed at understanding the molecular interactions of organophosphonate gaseous compounds with metal oxide surfaces is driven by the need to develop selective and sensitive sensors for the detection of toxic nerve agents.[1−23] Due to the highly toxic nature of nerve agents such as sarin and soman, research conducted at academic institutions has concentrated on benign analogues of these agents.

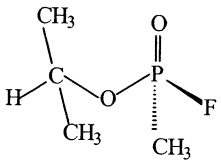

Sarin

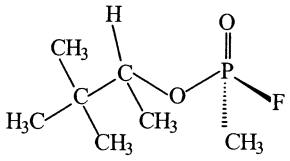

Soman

On the basis of a survey of the literature, dimethyl methyl phosphonate (DMMP) is by far the organophosphonate of choice for simulating the adsorption behavior of nerve agents on metal oxides.

On most oxides such as Al_2O_3,[11,24−26] TiO_2,[26−29] WO_3,[26,29] La_2O_3,[11] MgO,[11,16,20,26,30,31] Fe_2O_3,[11,21,32,33] and AgO,[14] DMMP adsorbs through the P═O functionality and decomposes via elimination of the methoxy groups at elevated temperatures producing a stable methyl phosphonate on the surface. This is in contrast to the adsorption behavior on silica, where DMMP adsorbs via a hydrogen bond between the methoxy modes and the surface SiOH groups and the subsequent evacuation at elevated temperature results in the complete desorption of intact DMMP molecules from the surface.[10]

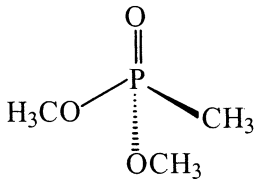

DMMP

The key attribute of DMMP, or any other simulant, is that they respond and behave as close as possible to the target agents. While the work on silica points to possible uses of this oxide for filtering and preconcentration schemes, it also revealed potential differences in the adsorption behavior of DMMP and the toxic agents. For example, our work with silica showed that the strength of adsorption of the organophosphonate depended on the number of alkoxy moieties attached to the central phosphorus atom.[10,34] DMMP, possessing two methoxy groups, adsorbs bifunctionally through two hydrogen bonds per molecule. As a result, DMMP is more strongly adsorbed on silica than organophosphonates such as sarin and soman that have only one alkoxy group that is hydrogen-bonded with the surface hydroxyl groups.

A second obvious difference between the structure of DMMP and sarin or soman is that the nerve agents have fluorine attached to the phosphorus atom. From a toxicological point of view, sarin reacts with water producing a phosphonic acid and HF,

* Corresponding author. Phone 207-581-2235. Fax 207-581-2255. E-mail: ctripp@maine.edu.
[†] Laboratory for Surface Science & Technology.
[‡] Department of Chemistry.

10.1021/jp014647x CCC: $22.00
Published on Web 08/17/2002

the phosphonic acid then combines with the hydroxyl groups of esterase enzymes producing an inactive phosphonate form of the enzyme. Hydrolysis of the nerve agent may be a key factor in WO_3-based sensors as the change in conductivity upon contact with DMMP is sensitive to the humidity level of the carrier gas stream. Moreover, recent infrared studies on WO_3 powders have shown that adsorbed water remains on the surface of WO_3 even after evacuation at a temperature of 350 °C.[35] Given that nerve agents such as sarin readily hydrolyze with water or the surface water on metal oxides,[36,37] the use of a nonhalogenated molecule such as DMMP may not be the best choice of molecules to mimic the sensor response of nerve agents.

In this paper, we use infrared spectroscopy to investigate the reaction of three phosphorus-containing compounds that vary in the number of chloro and methoxy groups attached to the central P atom with the surface of monoclinic WO_3 particles. Like the P−F group found in nerve agents, the P−Cl moiety should behave similarly in its interaction with surface sites or adsorbed water on the m-WO_3 surface.

Experimental Section

DMMP, TMP, and MDCP were purchased from Aldrich. All reagents were used as received and were transferred to evacuable glass bulbs using standard freeze−thaw cycles. The nanosized m-WO_3 powder was prepared in our laboratory using a sol−gel method.[38] The surface area of the powder was approximately 22 $m^2\ g^{-1}$ (BET N_2)

A detailed description of the infrared cell and procedures used for recording spectra are described elsewhere.[39] The m-WO_3 powder was dispersed as a thin film on a KBr window and mounted in the infrared cell. By using a thin film of the oxide, it is possible to extract modes due to adsorbed species in the region containing the strong W−O bulk modes. This is important when studying adsorbed phosphonates and phosphates because the characteristic C−O methoxy stretching modes overlap with the much stronger bulk modes. A thin film m-WO_3 was first evacuated either at room temperature, 150, or 400 °C followed by cooling to room temperature and are abbreviated WO_3(25), WO_3(150), and WO_3(400), respectively. After this pretreatment, a reference spectrum was then recorded through the thin WO_3 film. By using a WO_3 film as a reference, the absorbance spectrum (henceforth referred to as a difference spectrum) that is recorded after addition of the reactant contains both positive and negative bands. Positive bands are due to bonds that formed on the surface and negative bands represent bond removal from the surface.

To calculate the relative amount of adsorbed DMMP on the surface, the integrated intensity of the P−CH_3 mode at 1314 cm^{-1} is measured and divided by the intensity of the strong W−O band located at 830 cm^{-1}. The ratioed value is used in order to normalize band intensities to compensate for experiment-to-experiment variation in the amount of WO_3 probed by the infrared beam.

Addition of the vapor of each phosphorus compound was accomplished using standard vacuum line techniques. The difference spectrum was recorded after addition of excess vapor at room temperature for 1 min, followed by evacuation for 2 min. All spectra were recorded at room temperature on a Bomem MB-155S FTIR with a liquid-N_2-cooled MCT detector. Typically 200 scans were co-added at a resolution of 4 cm^{-1}.

Results and Discussion

The choice of the three evacuation temperatures of 25 °C, 150 °C, and 400 °C is based on results obtained for a previous dehydration and pyridine adsorption study.[35] It was found that about half of the total amount of adsorbed water is weakly adsorbed on the surface of WO_3 and easily removed with evacuation at room temperature. In contrast, there is little change in the amount of water (10%) between a WO_3(25) and WO_3(150) sample as about 40% of the total adsorbed water remains strongly bound to the surface at 150 °C. However, with evacuation at increasing temperatures above 200 °C the amount of strongly bound water decreases and is completely removed only after evacuation at 400 °C.

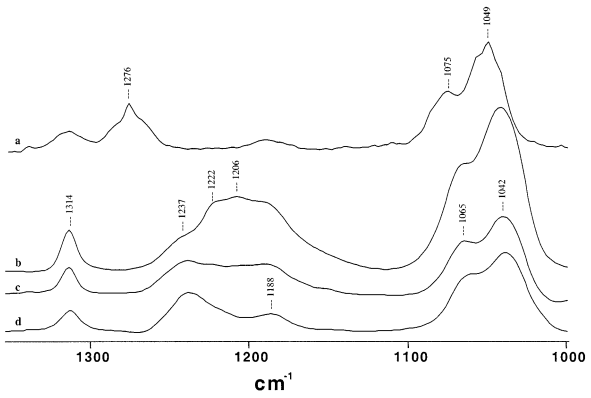

Figure 1. Infrared spectra of (a) gaseous DMMP and after addition of excess DMMP at room temperature for 1 min followed by evacuation for 2 min on (b) WO_3(25), (c) WO_3(150), and (d) WO_3(400).

In contrast to the dehydration behavior with evacuation temperature, pyridine adsorption studies showed that there is a marked difference in Lewis acidity between the WO_3(25) and WO_3(150) samples. There is a 50% reduction in the amount of adsorbed pyridine on the WO_3(150) sample compared to the amount of adsorbed pyridine on the WO_3(25) sample and this difference is due to a reduction in adsorption on the Lewis acid sites. On the other hand, the number of Brønsted sites slightly increases on WO_3(150) in comparison with WO_3(25). Furthermore, the adsorption of pyridine on WO_3(400) shows only a small (about 10%) change in the number of Lewis or Brønsted acid sites compared to the results obtained with a WO_3(150) sample.

The dehydration and pyridine adsorption data show that there is no connection between the dehydration behavior and the relative number of Lewis and Brønsted acid surface sites. The primary difference between WO_3(25) and WO_3(150) is a change in Lewis acid sites and not the amount of adsorbed water, whereas the primary difference between WO_3(150) and WO_3(400) is the removal of the adsorbed water with little change in either Lewis or Brønsted acidity.

Adsorption of DMMP and TMP on WO_3. The infrared spectra of adsorbed DMMP and TMP on separate WO_3 samples evacuated at 25, 150 and 400 °C along with the gas-phase spectra are shown in Figures 1 and 2, respectively. The gas-phase spectra are provided for comparative purposes and the assignments of the bands have been reported elsewhere.[10] Both DMMP and TMP are non-chlorine-containing organophosphorus simulants and the infrared spectra recorded after adsorption of these two compounds on the WO_3 powder show similar trends.

The O−CH_3 stretching modes in the region 1040−1075 cm^{-1} of the adsorbed species are slightly shifted to lower frequency compared to the corresponding bands of the gaseous DMMP and TMP. This is similar to the spectral data obtained for the adsorption of DMMP on WO_3[29] and TiO_2[27] and shows that there is no interaction between the methoxy groups and the surface. On the other hand, both DMMP and TMP adsorb on WO_3

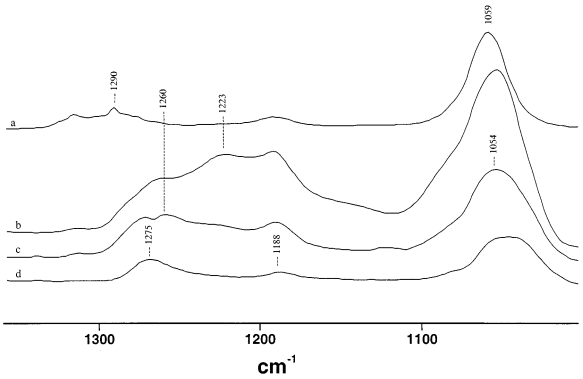

Figure 2. Infrared spectra of (a) gaseous TMP and after addition of excess TMP at room temperature for 1 min followed by evacuation for 2 min on (b) $WO_3(25)$, (c) $WO_3(150)$, and (d) $WO_3(400)$.

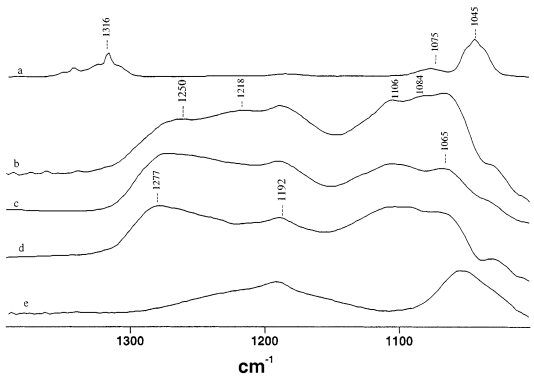

Figure 3. Infrared spectra of (a) gaseous MDCP and after addition of excess MDCP at room temperature for 1 min followed by evacuation for 2 min on (b) $WO_3(25)$, (c) $WO_3(150)$, and (d) $WO_3(400)$. Curve (e) is the infrared spectrum of the precipitate formed when MDCP is reacted with water.

through the P═O and the WO_3 surface sites as evidenced by the shift to lower frequency in the P═O stretching modes from the frequencies of their gaseous counterparts. In Figure 1b, three P═O stretching modes at 1237, 1222, and 1206 cm^{-1} (shifted from the gaseous DMMP by 39, 54, and 70 cm^{-1}, respectively) are evidence of the formation of three types of bonding between the P═O and sites on the $WO_3(25)$ surface. A fourth band at 1188 cm^{-1} in this region is assigned to the O−CH_3 rocking mode.[10,11,29]

The relative intensity of the three P═O bands vary with initial evacuation temperature at 25 °C, 150 °C, and 400 °C of the oxide and mirror the trends obtained for either dehydration of the oxide or adsorbed pyridine on WO_3 powders.[35] From a comparison of the relative intensity of the P−CH_3 band at 1314 cm^{-1} in Figure 1b−d, the amount of DMMP adsorbed on a $WO_3(25)$ sample is about twice the amount of DMMP adsorbed on either a $WO_3(150)$ or $WO_3(400)$ sample. This change in adsorbed amount is also accompanied by a change in the relative band intensities in the P═O stretching region. In Figure 1b−d, both bands at 1206 and 1222 cm^{-1} show changes in intensity, whereas the intensity of the band at 1237 cm^{-1} remains almost constant at all three pretreatment temperatures. The band at 1206 cm^{-1} shows the largest decrease in intensity between the 25 and 150 °C pretreated samples when compared to the reduction in intensity of the 1222 cm^{-1} band. We recall that there is only a small change in the level of adsorbed water between a $WO_3(25)$ and $WO_3(150)$ surface, whereas the latter surface exhibited a major decrease in the amount of pyridine coordinated to Lewis acid sites. Therefore, the infrared band at 1206 cm^{-1} is assigned to the DMMP adsorbed on WO_3 by forming a bond with a surface Lewis acid site (structure I).

The 1222 cm^{-1} band shows a slight reduction in intensity on a $WO_3(150)$ sample and a much larger decrease in intensity on the $WO_3(400)$ surface. The band at 1237 cm^{-1} remains constant irrespective of the sample evacuation temperature and is the dominate P═O mode on $WO_3(400)$. Thus, the 1222 cm^{-1} band mirrors the behavior of the dehydration of the oxide and we assign this band to adsorbed DMMP H-bonded with the strongly bound layer of water (structure II). The 1237 cm^{-1} band intensity follows the behavior expected for coordination to Brønsted acid sites (structure III) and is assigned accordingly. The three structures are shown in Scheme 1.

A trend similar that of DMMP is observed for TMP adsorbed on WO_3. The spectra in Figure 2b−d show three different bands at 1275, 1260, and 1223 cm^{-1} in the P═O stretching frequency region. Using the same arguments for assigning the P═O bands of adsorbed DMMP, the band at 1223 cm^{-1} (shift of 67 cm^{-1}) is assigned to the TMP adsorbed on the surface by forming an

SCHEME 1

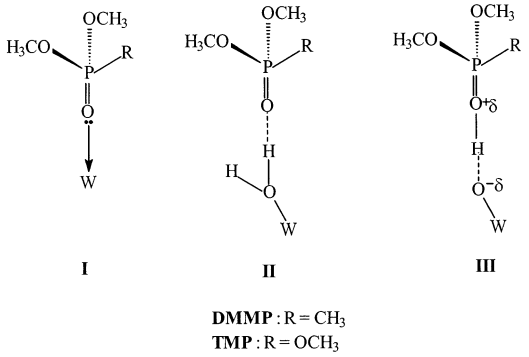

adduct with the surface Lewis sites. The peak at 1260 cm^{-1} is assigned to species adsorbed through a P═O group that is hydrogen-bonded to the surface water layer, and the band at 1275 cm^{-1} is assigned to species adsorbed through the P═O group with the surface Brønsted sites.

Adsorption of MDCP on WO_3. Figure 3a−d shows the infrared spectra of MDCP vapor (curve 3a) and MDCP adsorbed on the $WO_3(25)$, $WO_3(150)$, and $WO_3(400)$ samples (curves, 3b−d, respectively). There are similar trends in the behavior of the P═O modes for adsorbed MDCP with those obtained for adsorbed DMMP or TMP and clear differences in the trends observed for the O−C stretching methoxy modes. In Figure 3a, the P═O stretching mode at 1316 cm^{-1} for the gaseous MDCP now appear at 1277, 1250, and 1218 cm^{-1} when adsorbed on $WO_3(25)$. Furthermore, the two P═O modes at 1250 and 1218 cm^{-1} are reduced in intensity on both $WO_3(150)$ and $WO_3(400)$ relative to intensity of the band at 1277 cm^{-1} which remains almost constant in intensity at all three pretreatment temperatures. Given the similarities to DMMP and TMP adsorption, the 1277 cm^{-1} band is assigned to adsorption of the P═O to WO_3 Brønsted sites, whereas the bands at 1250 and 1218 cm^{-1} are assigned to the P═O functionality hydrogen-bonded to the adsorbed water and coordinated to the Lewis site of the surface, respectively.

The gas-phase spectrum for MDCP shows a methoxy rocking mode at 1188 cm^{-1} along with two (υ_{O-CH3}) methoxy stretching bands at 1075 and 1045 cm^{-1} (see Figure 3a). With adsorption of MDCP on $WO_3(25)$, a band at 1192 cm^{-1} along with three broad bands at 1106, 1084, and 1065 cm^{-1} are observed. This is a completely different trend from the results found for DMMP and TMP adsorbed on WO_3. For both DMMP and TMP, there was almost no difference in the shape and frequency of the

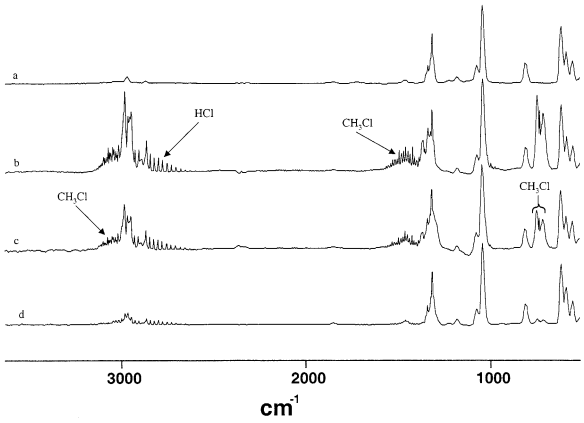

Figure 4. Infrared spectra of the vapor phase after addition of MDCP vapor for 5 min to (a) an evacuated gas cell only, (b) WO_3(25) thin film, (c) WO_3(150) thin film, and (d) WO_3(400) thin film.

methoxy stretching modes between the gaseous and adsorbed molecules. One possible explanation for this difference with adsorbed MDCP is that the methoxy group of MDCP reacts with the surface or the adsorbed water. In this case, none of the three bands at 1106, 1084, and 1065 cm^{-1} would be due to methoxy stretching modes. However, the CH_3 stretching modes at 2963 and 2862 cm^{-1} are detected and thus the adsorbed species (or at least one of the adsorbed species) does contain methoxy moieties. Therefore, at least one of the three bands at 1106, 1084, and 1065 cm^{-1} in curve 3b should be assigned for the methoxy stretching modes.

The most likely explanation for an upward shift in the methoxy C−O stretching mode is that the MDCP is hydrolyzed on the surface by the adsorbed water layer or in the gas phase with the water expelled from the surface. Hydrolysis by water is the most likely explanation as the P−Cl modes of gaseous MDCP do not appear in the spectrum of MDCP adsorbed on WO_3(25) (spectrum not shown). There are several pieces of evidence showing that the adsorbed water plays a significant role in the hydrolysis process. Figure 4 shows the infrared spectra of MDCP vapor in the gas cell for 5 min without the WO_3 surface present (Figure 4a) and the exposure of MDCP into the gas cell that contained WO_3(25), WO_3(150), and WO_3-(400) (see Figure 4b−d, respectively). Clearly, the presence of a hydrated WO_3 surface enhances the MDCP hydrolysis as seen by the formation of HCl vibrational modes between 2650 and 3100 cm^{-1} as well as vibrational−rotational bands at 3000−3200, 1380−1570, and 750−710 cm^{-1} that are due to the formation of gaseous CH_3Cl. In Figure 4, the relative amount of the HCl and CH_3Cl decreases with increasing pretreatment temperature of WO_3. Specifically, the relative amount of CH_3-Cl formed when MDCP was exposed to the WO_3(25) surface for 5 min is larger than the relative amount of CH_3Cl formed upon the exposure of MDCP vapor to WO_3(150) and WO_3-(400) for 5 min by 2 and 14 times, respectively. Moreover, there is a 60% reduction in intensity of the bending water mode at 1610 cm^{-1} when MDCP is added to WO_3(25) and a corresponding 26% reduction in this same band occurs on WO_3(150). In contrast, there is no reduction in intensity of the water bending mode and therefore no interaction between adsorbed DMMP or TMP and the surface adsorbed water on WO_3. While it is clear that the adsorbed water is a reservoir for creating hydrolyzed product, it is not certain whether the hydrolysis occurs with the adsorbed water at the surface or in the vapor phase with water displaced from the surface.

Even on a WO_3(400) surface that contains no adsorbed water, there are broad bands in the 1150−1050 cm^{-1} region, HCl and CH_3Cl are detected in the gas phase and there are no P−Cl modes observed. In this case, we believe this reflects the ease with which MDCP readily hydrolyzes with water vapor in the system. In the stock MDCP there are traces of HCl and CH_3Cl in the gas-phase spectrum and GC-MS analysis of the MDCP show the formation of HCl, CH_3Cl, $(CH_3O)PO(OH)Cl$, (CH_3O)-$PO(OH)_2$, and $PO(OH)_3$. Scheme 2 shows the products that form after the hydrolysis of MDCP as identified by GC-MS. Therefore, displacement of water on the surface into the vapor phase could occur through adsorption of one of the hydrolyzed gaseous MDCP molecules. In separate experiments, the exposure of gaseous MDCP vapor to water vapor results in the immediate and complete conversion to the same gaseous products as determined by GC-MS analysis. When this gaseous mixture is added to a WO_3(400), a spectrum similar to Figure 3d is obtained. In this case there is no MDCP vapor but only the hydrolyzed products. In the end, the observed changes in the relative amounts of MDCP hydrolysis in the presence of the WO_3 thin films evacuated at different temperatures indicate that adsorbed water plays a significant role in the hydrolysis of MDCP.

SCHEME 2

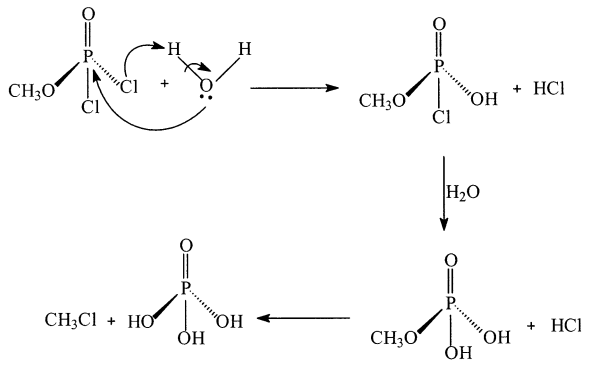

We anticipate a range of adsorbed species given the variety of partially and fully hydrolyzed phosphorus-containing gaseous compounds exposed to the WO_3 surface. From spectroscopic arguments, the substitution of P−Cl groups with either POH or a P−O−P network would lead to a shift to higher frequency in the O−C methoxy stretching mode. However, it is unlikely that some of the features between 1150 and 1050 cm^{-1} are due to POH bending modes as they typically appear below 1000 cm^{-1}. This conclusion is supported by a separate experiment in which a WO_3(25) sample was exposed to D_2O vapor. This procedure leads to complete deuteration of the adsorbed water and surface hydroxyl groups.[35] When MDCP is added to the deuterated sample, there is no shift in the bands at 1084 and 1065 cm^{-1} whereas the band at 1106 cm^{-1} broadens and is centered at a higher frequency of 1112 cm^{-1}. Given the results of the deuterated sample, the most likely explanation for the broad band structure located between 1200 and 1000 cm^{-1} is that it is due to a mixture of O−C methoxy and P−O−P modes. Given the shift in the P═O stretching modes, the adsorbed species is anchored to the surface through bonds with the P═O groups.

The assignment of bands due to P−O−P is consistent with the spectrum of known compounds. The infrared spectrum obtained for a solution of sodium methyl phosphate shows bands at 1085, 1050, and 972 cm^{-1} that are assigned to various P−O modes associated with CH_3PO_32- ions.[40] Furthermore, when MDCP liquid is exposed to water, a precipitate quickly forms. The infrared spectrum of the precipitate is shown in Figure 3e

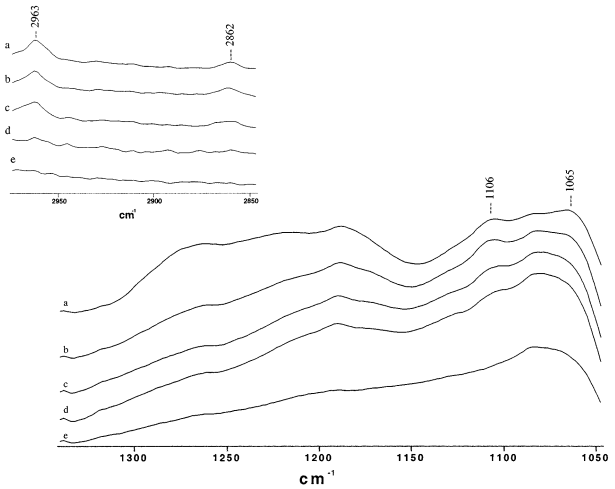

Figure 5. (a) Infrared spectra of adsorbed MDCP on WO_3(25) followed by evacuation at (b) 100 °C, then (c) 200 °C, then (d) 300 °C, and then (e) 400 °C.

and shows two characteristic bands at 1192 and 1065 cm^{-1} that are most likely due to an adsorbed phosphate.

To further aid in determining the nature of the adsorbed MDCP, a WO_3(25) sample exposed to MDCP was then evacuated at increasing temperatures. The spectra obtained are shown in Figure 5. Under these evacuation conditions, it has been shown that adsorbed DMMP on WO_3, TiO_2[29] and Al_2O_3[11] loses its methoxy groups above 200 °C and gives rise to an adsorbed methyl phosphonate attached to the surface. Spectroscopically, the CH_3 and O−C stretching modes and the various P═O modes decrease and are replaced by two broad bands at 1190 and 1060 cm^{-1} when the DMMP-treated WO_3, TiO_2, or Al_2O_3 is evacuated above 200 °C. A similar trend is obtained with evacuation at elevated temperatures of adsorbed MDCP on WO_3(25). In Figure 5, the C−H stretching modes at 2963 and 2862 cm^{-1} are eliminated by evacuation between 200 and 300 °C and this is accompanied by a decrease in the band at 1106 cm^{-1} (O−C stretching mode) and elimination of the various P═O modes at 1277, 1250, and 1218 cm^{-1}. Upon removal of the methoxy groups, two broad bands centered near 1190 and 1065 cm^{-1} remain and these are characteristic of phosphates on the surface.

In summary, there is a clear difference in the type of adsorbed species formed when chloro- and non-chloro-containing organophosphorus compounds come in contact with WO_3 surfaces. This difference is due to hydrolysis of the chloro-containing phosphate with the adsorbed water layer or with water vapor replaced from the surface. However, the presence of hydrolyzed material does not alter the mode of attachment as MDCP, DMMP, and TMP adsorb via the P═O group with surface sites.

Conclusion

An infrared study of DMMP, TMP, and MDCP adsorption on WO_3 high surface area powders shows that all phosphonates and phosphates adsorb on WO_3 via the P═O functionality with Lewis and Brønsted surface acid sites and with the adsorbed layer of water. The relative number of molecules bound on different surface sites depends on the initial evacuation temperature of the WO_3 surface as this alters the relative number of the Lewis and Brønsted acid surface sites along with the amount of adsorbed water or water vapor. The main difference between the chlorinated phosphate MDCP and non-chlorinated DMMP or TMP is that the MDCP readily hydrolyzes with water vapor or the adsorbed layer of water. Given that both sarin and soman have been shown to hydrolyze to form covalently attached methyl phosphates on various metal oxides,[36] the use of MDCP should be a better simulant for studying humidity effects in sensors than the more commonly used simulant, DMMP.

Acknowledgment. This work was supported by the Department of the Navy, Naval Surface Warfare Center, Dahlgren Division, Grant N00178-1-9002.

References and Notes

(1) Lunkenheimer, K.; Haage, K.; Hirte, R. *Langmuir* **1999**, *15*, 1052.
(2) Bertilsson, L.; Potje-Kamloth, K.; Liess, H. D.; Liedberg, B. *Langmuir* **1998**, *15*, 1128.
(3) Henderson, M. A.; Jin, T.; White, J. M. *J. Phys. Chem.* **1986**, *90*, 4607.
(4) Moravie, R. M.; Froment, F.; Corset, J. *Spectrochim. Acta* **1989**, *45A*, 1015.
(5) Elbrecht, L.; Catanescu, R.; Zacheja, J.; Binder, J. *Sens. Actuators, A* **1997**, *61*, 374.
(6) Hedge, R. I.; Greenlief, C. M.; White, J. M. *J. Phys. Chem.* **1985**, *89*, 2886.
(7) Smentkowski, V. S.; Hagans, P.; Yates, J. T., Jr. *J. Phys. Chem.* **1988**, *92*, 6351.
(8) Sohn, H.; Létant, S.; Sailor, M. J.; Trogler, W. C. *J. Am. Chem. Soc.* **2000**, *122*, 5399.
(9) Gay, I. D.; McFarlan, A. J.; Morrow, B. A. *J. Phys. Chem.* **1991**, *95*, 1360.
(10) Kanan, S. M.; Tripp, C. P. *Langmuir* **2001**, *17*, 2213.
(11) Mitchell, M. B.; Sheinker, V. N.; Mintz, E. A. *J. Phys. Chem.* **1997**, *101*, 11192.
(12) Bertilsson, L.; Engquist, I.; Liedberg, B. *J. Phys. Chem. B* **1997**, *101*, 6021.
(13) Oh, S. W.; Kim, Y. H.; Yoo, D. J.; Oh, S. M.; Park, S. J. *Sens. Actuators, B* **1993**, *13*−*14*, 400.
(14) Taranenko, N.; Alarie, J. P.; Stokes, D. L.; Vo-Dinh, T. *J. Raman Spectrosc.* **1996**, *27*, 379.
(15) Bertilsson, L.; Karin, P. K.; Liess, H. D. *J. Phys. Chem. B* **1998**, *102*, 1260.
(16) Bertilsson, L.; Potje-Kamloth, K.; Liess, H. D. *Langmuir* **1999**, *15*, 1128.
(17) Henderson, M. A.; White, J. M. *J. Am. Chem. Soc.* **1988**, *110*, 6939.
(18) Lee, K. Y.; Houalla, M.; Hercules, D. M.; Hall, W. K. *J. Catal.* **1994**, *145*, 223.
(19) Bertilsson, L.; Potje-Kamloth, K.; Liess, H. D.; Engquist, I.; Liedberg, B. *J. Phys. Chem.* **1998**, *102*, 1260.
(20) Li, Y. X.; Klabunde, K. J. *Langmuir* **1991**, *7*, 1388.
(21) Hedge, R. I.; White, J. M. *Appl. Surf. Sci.* **1987**, *28*, 1.
(22) Macdonald, M. A.; Jayaweera, T. M.; Gouldin, F. C. *Combust. Flame* **1999**, *116*, 166.
(23) Korobeinichev, O. P.; Ilyin, S. B.; Shvartsberg, V. M.; Chernov, A. A.; Bolshova, T. A. *Combust. Flame* **1999**, *121*, 593.
(24) Cao, L.; Segal, S. R.; Suib, S. L.; Tang, X.; Satyapal, S. *J. Catal.* **2000**, *194*, 61.
(25) Templeton, M. K.; Weinberg, W. H. *J. Am. Chem. Soc.* **1985**, *107*, 774.
(26) Blajeni-Aurian, B.; Boucher, M. M. *Langmuir* **1989**, *5*, 170.
(27) Rusu, C. N.; Yates, J. T., Jr. *J. Phys. Chem. B* **2000**, *104*, 12292.
(28) Obee, T. N.; Satyapal, S. *J. Photochem. Photobiol., A* **1998**, *118*, 45.
(29) Kim, C. S.; Lad, R. J.; Tripp, C. P. *Sens. Acuators, A* **2001**, 76, 442.
(30) Zhanpeisov, N. U.; Zhidomirov, G. M.; Yudanov, I. V.; Klabunde, K. J. *J. Phys. Chem.* **1994**, *98*, 10032.
(31) Li, Y. X.; Schlup, J. R.; Klabunde, K. J. *Langmuir* **1991**, *7*, 1394.
(32) Henderson, M. A.; Jin, T.; White, J. M. *J. Phys. Chem.* **1986**, *90*, 4607.
(33) Tesfai, T. M.; Sheinker, V. N.; Mitchell, M. B. *J. Phys. Chem. B* **1998**, *102*, 7299.
(34) Kanan, S. M.; Tripp, C. P. *Langmuir* **2002**, *18*, 722.
(35) Kanan, S. M.; Lu, Z.; Cox, J. K.; Bernhardt, G.; Tripp, C. P. *Langmuir* **2002**, *18*, 1707.
(36) Wagner, G. W.; Procell, L. R.; O'Connor, R. J.; Munavalli, S.; Carnes, C. L.; Kapoor, P. N.; Klabunde, K. J. *J. Am. Chem. Soc.* **2001**, *123*, 1636.
(37) Wagner, G. W.; Koper, O. R.; Lucas, E.; Decker, S.; Klabunde, K. J. *J. Phys. Chem. B* **2000**, *104*, 5118.
(38) Lu, Z.; Kanan, S. M.; Tripp, C. P. *J. Mater. Chem.* **2002**, *12*, 983.
(39) Tripp, C. P.; Hair, M. L. *Langmuir* **1991**, *7*, 923.
(40) Bellamy, L. J. *The Infrared Spectra of Complex Molecules*.; Chapman and Hall Ltd.: Thetford, U.K., 1975.